

NASA TM-86701

NASA Technical Memorandum 86701

NASA-TM-86701 19850015393

---

# Estimating Unsteady Aerodynamic Forces on a Cascade in a Three-Dimensional Turbulence Field

---

Tom Norman and Wayne Johnson

---

NOT TO BE TAKEN FROM THIS ROOM

March 1985

LIBRARY COPY

APR 29 1985

LANGLEY RESEARCH CENTER  
LIBRARY, NASA  
HAMPTON, VIRGINIA



---

# **Estimating Unsteady Aerodynamic Forces on a Cascade in a Three-Dimensional Turbulence Field**

---

Tom Norman  
Wayne Johnson, Ames Research Center, Moffett Field, California

March 1985



National Aeronautics and  
Space Administration

**Ames Research Center**  
Moffett Field, California 94035

---

## NOMENCLATURE

A	vane set area, $\text{m}^2$
$a_1, a_2, a_3, a_4$	"effective" lift or drag curve slope
$C_d, C_l$	drag and lift constants, $\text{N}\cdot\text{sec}/\text{m}^2$
c	vane chord, $\text{m}$
$D_G$	global vane set drag, $\text{N}$
d	section drag, $\text{N}/\text{m}$
$E(v^*)$	energy spectrum function $(\text{m/sec})^2 \text{ m}$
$k, k_1, k_2$	reduced frequencies
H	total height of one vane, $\text{m}$
L	characteristic length scale for turbulence, $\text{m}$
$L_G$	global vane set lift, $\text{N}$
$\lambda$	section lift, $\text{N}/\text{m}$
N	number of vanes in vane set
R	correlation function
$r_n$	velocity ratio $(V/V_{0_{\max}})$ across vane set
S	spectral function
$s(x)$	velocity ratio $(V/V_{0_{\max}})$ along vane span
$T(k_1, k_2)$	extended Sears function
TI	turbulence intensity
t	time, sec
u	axial velocity, $\text{m/sec}$
V	free stream velocity, $\text{m/sec}$
$V_0$	time averaged velocity of flow parallel to tunnel centerline, $\text{m/sec}$

$v_z$	velocity perpendicular to vane set stagger line, m/sec
$w$	lateral velocity, m/sec
$x$	vertical (vane span) coordinate, m
$y$	streamwise coordinate, m
$z$	total distance along stagger line, m
$z$	cross-stream coordinate, m
$\beta$	angle between free stream velocity vector and line perpendicular to stagger line, rad
$\beta^*$	angle between free stream and tunnel centerline, rad
$\eta$	cross-stream separation distance, m
$\eta_d$	viscous drag coefficient
$\theta_{ij}$	three-dimensional turbulent velocity power spectrum, $(\text{m/sec})^2 \text{ m}^3$
$\theta_1$	stagger angle, rad
$\mu$	wave number of cross-stream velocity fluctuations, $\text{m}^{-1}$
$\nu$	wave number of spanwise velocity fluctuations, $\text{m}^{-1}$
$\nu^*$	wave number magnitude, $\text{m}^{-1}$
$\nu_1, \nu_2, \nu_3$	wave number components, $\text{m}^{-1}$
$\xi$	spanwise separation distance, m
$\rho$	air density, $\text{kg/m}^3$
$\sigma$	root-mean-squared (rms) value
$\tau$	time delay, sec
$\Phi_2$	spanwise correlation function, m
$\Phi_3$	vane to vane correlation function
$\phi_{ij}$	one-dimensional turbulent velocity power spectrum, $(\text{m/sec})^2 \text{ m}$
$\psi_{ij}$	two-dimensional turbulent velocity power spectrum, $(\text{m/sec})^2 \text{ m}^2$

$\Omega_b$  characteristic "break" frequency, rad/sec  
 $\omega$  frequency of axial velocity fluctuations, rad/sec

Subscripts

$D_G$  global drag  
 $d$  section drag  
 $L_G$  global lift  
 $l$  section lift  
 $m$  mean value  
 $u$  axial velocity  
 $w$  lateral velocity  
1 conditions upstream of vane set  
2 conditions downstream of vane set

## SUMMARY

An analytical method has been developed to estimate the unsteady aerodynamic forces caused by flow field turbulence on a wind tunnel turning-vane cascade system (vane set). This method approximates dynamic lift and drag by linearly perturbing the appropriate steady-state force equations, assuming that the dynamic loads are due only to free-stream turbulence and that this turbulence is homogeneous, isotropic, and Gaussian. Correlation and unsteady aerodynamic effects are also incorporated into the analytical model. Using these assumptions, equations relating dynamic lift and drag to flow turbulence, mean velocity, and vane set geometry are derived. From these equations, estimates for the power spectra and rms (root-mean-squared value,  $\sigma$ ) loading of both lift and drag can be determined.

## INTRODUCTION

NASA Ames Research Center currently has a modification project under way to expand the capabilities and improve the aerodynamic characteristics of its 40- by 80-Foot Wind Tunnel. Various aspects of this project have been reported in earlier papers, with Corsiglia et al. (ref. 1), being the most recent. One modification already completed is the installation of a new drive system, which increased the maximum attainable speed in the existing closed circuit tunnel from 100 to 150 m/sec (200 to 300 knots). Also, a nonreturn leg with a 24- by 37-m (80- by 120-ft) test section has been added. This new tunnel, which shares the drive system with the closed circuit facility, is designed for a maximum test section velocity of 50 m/sec (100 knots). A plan view of this entire facility, called the National Full-Scale Aerodynamic Complex (NFAC), is shown in figure 1.

Located inside the NFAC are eight sets of turning-vane cascades (vane sets). These vane sets, built to turn air efficiently around corners and provide acceptable flow quality throughout the wind tunnel circuit, were originally designed to withstand the aerodynamic loads occurring at the maximum tunnel velocity of 100 m/sec. To ensure the structural integrity of these vane sets at the new design's maximum velocity, it became necessary to develop a theoretical method for estimating the aerodynamic loads. Two types of aerodynamic loads were required to test individual vane strength and vane superstructure strength. Local loads were the spanwise loads over one vane section used to determine the structural strength requirements of the individual vanes. Global loads were the net aerodynamic forces on an entire vane set used in the structural analysis of the vane set superstructure.

It is important to realize that the NFAC is not a completely new facility. As a result, very conservative loads estimates could cause the structural analysis to incorrectly indicate a need for the reinforcement or renovation of the existing structures. Thus it was necessary to provide accurate estimates of loads to ensure structural integrity and to minimize cost. Given this accuracy requirement, analytical procedures for estimating both steady and unsteady vane set forces were derived. The method used in estimating the dynamic loads is presented in this report. Steady-state load estimation procedures will be published separately.

### DYNAMIC FORCE EQUATIONS

The development of the dynamic loads estimation procedure began with the assumption that dynamic forces could be estimated by linearly perturbing the appropriate steady state force equations. For a turning-vane cascade system with uniform inflow and outflow and no steady vertical velocity component, the global vane set lift and drag are (ref. 2)

$$L_G = \rho V_{z_1}^2 A (\tan \beta_1 - \tan \beta_2) \quad (1)$$

$$D_G = \frac{1}{2} \rho V_{z_1}^2 A (\tan^2 \beta_2 - \tan^2 \beta_1) + \frac{1}{2} \rho V_1^2 n_d A \quad (2)$$

where

$$V_{z_1} = V_1 \cos \beta_1 \quad (3)$$

the area of the vane set is  $A$ , and  $n_d$  is the viscous-loss coefficient. The sign conventions used for lift and drag ( $L_G$ ,  $D_G$ ), for the pertinent velocities ( $V_{z_1}$ ,  $V_1$ ), and for the inflow and outflow angles ( $\beta_1$ ,  $\beta_2$ ) are shown in figure 2.<sup>1</sup>

By dividing equations (1) and (2) by the total span of the vanes and then incorporating equation (3), the sectional lift and drag equations can be derived

$$l = \rho V_1^2 \frac{Z}{N} \cos^2 \beta_1 (\tan \beta_1 - \tan \beta_2) \quad (4)$$

$$d = \frac{1}{2} \rho V_1^2 \frac{Z}{N} (\cos^2 \beta_1 \tan^2 \beta_2 - \sin^2 \beta_1 + n_d) \quad (5)$$

where  $Z$  is the total distance along the vane set stagger line and  $Z/N$  is the distance between vanes.

---

<sup>1</sup>Note that the direction of drag is opposite to that shown in reference 2.

Dynamic force equations can then be derived by linearly perturbing equations (4) and (5) about the variables  $V_1$  and  $\beta_1$ , with  $\beta_2$  assumed constant. This analysis yields the following equations

$$\delta L = b_1 V_{1m} \delta V_1 + b_2 V_{1m}^2 \delta \beta_1 \quad (6)$$

$$\delta D = b_3 V_{1m} \delta V_1 + b_4 V_{1m}^2 \delta \beta_1 \quad (7)$$

where the subscript  $m$  designates a mean (steady state) value, and

$$b_1 = 2\rho \frac{Z}{N} \cos^2 \beta_{1m} \left( \tan \beta_{1m} - \tan \beta_2 \right) \quad (8)$$

$$b_2 = \rho \frac{Z}{N} \left( \cos^2 \beta_{1m} - \sin^2 \beta_{1m} + 2 \cos \beta_{1m} \sin \beta_{1m} \tan \beta_2 \right) \quad (9)$$

$$b_3 = \rho \frac{Z}{N} \left( \cos^2 \beta_{1m} \tan^2 \beta_2 - \sin^2 \beta_{1m} + n_L \right) \quad (10)$$

$$b_4 = \rho \frac{Z}{N} \left( -\cos \beta_{1m} \sin \beta_{1m} \tan^2 \beta_2 - \cos \beta_{1m} \sin \beta_{1m} \right) \quad (11)$$

From figure 2, it follows that the axial and lateral inflow velocities ( $u, w$ ) can be defined as

$$u = V_1 \cos \beta^* \quad (12)$$

$$w = V_1 \sin \beta^* \quad (13)$$

where  $\beta^* = \beta_1 - \theta_1$ . Perturbing these equations yields

$$\delta u = \delta V_1 \cos \beta_m^* - w_m \delta \beta_1 \quad (14)$$

$$\delta w = \delta V_1 \sin \beta_m^* + u_m \delta \beta_1 \quad (15)$$

Solving these two equations for  $\delta \beta_1$  and  $\delta V_1$ , and substituting them into equations (6) and (7), the fluctuating lift and drag can now be expressed as

$$\delta L = C_{L_w} \delta w + C_{L_u} \delta u \quad (16)$$

$$\delta D = C_{D_w} \delta w + C_{D_u} \delta u \quad (17)$$

where

$$C_{L_w} = \frac{1}{2} \rho V_0^2 c a_1 \quad (18)$$

$$C_{L_u} = \frac{1}{2} \rho V_0^2 c a_2 \quad (19)$$

$$C_{D_w} = \frac{1}{2} \rho V_0^2 c a_3 \quad (20)$$

$$C_{D_u} = \frac{1}{2} \rho V_0^2 c a_4 \quad (21)$$

$$a_1 = (b_1 w_m + b_2 u_m) / \left( \frac{1}{2} \rho V_0^2 c \right) \quad (22)$$

$$a_2 = (b_1 u_m - b_2 w_m) / \left( \frac{1}{2} \rho V_0^2 c \right) \quad (23)$$

$$a_3 = (b_3 w_m + b_4 u_m) / \left( \frac{1}{2} \rho V_0^2 c \right) \quad (24)$$

$$a_4 = (b_3 u_m - b_4 w_m) / \left( \frac{1}{2} \rho V_0^2 c \right) \quad (25)$$

$$u_m = V_0 \cos \theta_1 \cos \beta_m^* / \cos \beta_{1m} \quad (26)$$

$$w_m = V_0 \cos \theta_1 \sin \beta_m^* / \cos \beta_{1m} \quad (27)$$

$$V_0 = V_{1m} \cos \beta_{1m} / \cos \theta_1 \quad (28)$$

## UNSTEADY AERODYNAMICS AND THREE-DIMENSIONAL EFFECTS

Equations (16) and (17) are estimates of unsteady sectional lift and drag using a quasi-steady airfoil approach and assuming that lift and drag respond instantaneously to flow field changes. It is known, however, that the lift on an airfoil in a fluctuating flow field does not change instantaneously, but is dependent on the frequency of that fluctuation (ref. 3). This frequency dependency can be described by a transfer function relating lift to angle of attack ( $\delta\theta_1$ ). It is also known that a transfer function exists between the lift and the pulsating flow velocity,  $\delta V_1$  (ref. 4). For this analysis, we used a single transfer function for both effects. It was also assumed that this lift transfer function could be applied to

dynamic drag. This latter assumption is reasonable for momentum drag, since it is dependent solely on angle of attack. The applicability of this transfer function to viscous drag ( $\eta_d$ ), however, is questionable and thus it must be assumed that  $\eta_d$  is small compared to momentum drag. Using these assumptions, equations (16) and (17) become

$$\delta L = C_{L_w} \delta w T + C_{L_u} \delta u T \quad (29)$$

$$\delta d = C_{d_w} \delta w T + C_{d_u} \delta u T \quad (30)$$

where Filotas' approximation (ref. 5) was used for the extended Sears function ( $T$ ). This approximation assumes a sinusoidally varying velocity gust engaging a wing of infinite aspect ratio (no wall effects). It incorporates unsteady effects (Sears function) and three-dimensional (3-D) effects due to the gust hitting the vane obliquely. Any possible cascade effects on  $T$  were ignored. The transfer function is defined as

$$|T(k_1, k_2)|^2 = \left[ 1 + \pi k \left( 1 + \left( \frac{k_1}{k} \right)^2 + \pi |k_2| \right) \right]^{-1} \quad (31)$$

where the reduced frequencies are

$$k_1 = \omega c / 2V_0 \quad (32)$$

$$k_2 = v c / 2 \quad (33)$$

$$k^2 = k_1^2 + k_2^2 \quad (34)$$

The frequency of the axial velocity fluctuation is  $\omega$  and the wave number of the lateral velocity fluctuation is  $v$ . The effects of  $k_1$  and  $k_2$  on  $T$  can be seen in figure 3.

Equations (29) and (30) give the dynamic lift and drag loads at one frequency. Assuming that velocity fluctuations (turbulence) can be described as a linear superposition of sinusoidal components, it follows that lift and drag can be expressed in terms of spectra incorporating all frequencies. Through Fourier analysis, it can be shown that the power spectra of lift and drag become

$$S_L(\omega, v, \mu) = C_{L_w}^2 |T|^2 S_w(\omega, v, \mu) + C_{L_u}^2 |T|^2 S_u(\omega, v, \mu) + 2C_{L_u} C_{L_w} |T|^2 \mathcal{R}(S_{uw}(\omega, v, \mu)) \quad (35)$$

$$S_d(\omega, v, \mu) = C_{d_w}^2 |T|^2 S_w(\omega, v, \mu) + C_{d_u}^2 |T|^2 S_u(\omega, v, \mu) + 2C_{d_u} C_{d_w} |T|^2 \mathcal{R}(S_{uw}(\omega, v, \mu)) \quad (36)$$

where  $S_w$  is the lateral,  $S_u$  is the axial, and  $S_{uw}$  is the cross-turbulent velocity spectra. The third independent variable in these equations ( $\mu$ ) is defined as the wave number for the vertical velocity fluctuation. The form of these velocity spectra will be discussed later.

### GLOBAL DYNAMIC LOADS ON A VANE SET

As mentioned previously, one goal of this analysis was to estimate the global dynamic loads on a vane set. One way of presenting these global loads is with one-dimensional power spectra and their associated rms integrated loads. For global lift, this one-dimensional spectrum can be defined as

$$S_{L_G}(\omega) = \frac{1}{2\pi} \int_{-\infty}^{+\infty} R_{L_G}(\tau) e^{-i\omega\tau} d\tau \quad (37)$$

where  $R_{L_G}$  is the correlation function for global lift with time delay  $\tau$ . This correlation function is defined as

$$R_{L_G}(\tau) = E[L_G(t)L_G(t + \tau)] \quad (38)$$

where  $E[ ]$  is the expected value and  $L_G$  is global lift.

It is possible to get a more useful form for the global correlation function by making use of some definitions. First, global lift can be defined as the summation of lift of all the individual vanes, such that

$$L_G = \sum_{n=1}^N L_n \quad (39)$$

where  $L_n$  is the lift on one vane. By substituting this expression into equation (38) the global and one vane correlation functions are related by

$$R_{L_G}(\tau) = \sum_{m=1}^N \sum_{n=1}^N R_{L_{mn}}(\tau, n) \quad (40)$$

where  $R_{L_{mn}}$  is the one vane lift correlation function at time delay  $\tau$  and lateral vane separation  $n = z_n - z_m$ .

A second definition states that the lift on one vane is a function of section lift such that

$$L_n = \int_0^H \ell dx \quad (41)$$

where  $H$  is equal to the total vane height. It follows from this relationship that

$$R_{L_{mn}}(\tau, n) = \int_0^{H_2} \int_0^{H_1} R_{\ell_{mn}}(\tau, n, \xi) dx_1 dx_2 \quad (42)$$

where  $R_{\ell_{mn}}$  is the section lift correlation function at time delay  $\tau$ , lateral vane separation  $n$ , and vertical separation  $\xi = x_1 - x_2$ . Using equation (29),  $R_{L_{mn}}$  subsequently becomes a function of the lateral and axial velocity correlations (the cross correlation of the velocities,  $R_{uw}$ , is zero for isotropic turbulence).

$$\begin{aligned} R_{L_{mn}}(\tau, n) &= \int_0^{H_2} \int_0^{H_1} C_{\ell_w m} C_{\ell_w n} |T|^2 R_w(\tau, n, \xi) dx_1 dx_2 \\ &+ \int_0^{H_2} \int_0^{H_1} C_{\ell_u m} C_{\ell_u n} |T|^2 R_u(\tau, n, \xi) dx_1 dx_2 \end{aligned} \quad (43)$$

Note that unlike the global lift correlation function ( $R_{L_G}$ ), which is dependent only on time separation ( $\tau$ ), the turbulence correlation functions are dependent on separations in three dimensions ( $\tau, n, \xi$ ). The lateral-turbulent velocity correlation function ( $R_w$ ) can be defined as the Fourier transform of its respective power spectrum, such that

$$R_w(\tau, n, \xi) = \iiint_{-\infty}^{+\infty} S_w(\omega^*, v, \mu) e^{i\omega^* r + i\nu\xi + i\mu n} d\omega^* dv d\mu \quad (44)$$

The axial correlation function,  $R_u$ , can be defined similarly.

Incorporating nonuniform velocity profiles into the calculations can be done easily at this point by including variables in equations (18)-(21). For example

$$C_{\ell_w} = \frac{1}{2} \rho V_0 \max_{\text{max}} c a_1 r_n s(x) \quad (45)$$

where  $V_{0_{\max}}$  is the peak axial velocity,  $r_n$  is the velocity ratio ( $V/V_{0_{\max}}$ ) at each vane  $n$ , and  $s(x)$  is the velocity ratio along the vane height. For simplicity, it is assumed that the  $r_n$  profile is similar for all vane heights, and the  $s(x)$  profile is similar for all vanes.

By combining equations (40), (43), (44), and (45), equation (37) becomes

$$S_{L_G}(\omega) = \frac{1}{2\pi} \int_{-\infty}^{+\infty} \sum_{m=1}^N \sum_{n=1}^N \int_0^{H_2} \int_0^{H_1} s(x_1)s(x_2)r_m r_n \times \left[ \iiint_{-\infty}^{+\infty} S_g(\omega^*, v, \mu) e^{-i(\omega - \omega^*)\tau + iv\xi + i\mu\eta} dv d\mu \right] dx_1 dx_2 d\tau \quad (46)$$

However, it can be shown that

$$\frac{1}{2\pi} \iint_{-\infty}^{+\infty} S_g(\omega^*, v, \mu) e^{-i(\omega - \omega^*)\tau} d\omega^* d\tau = \int_{-\infty}^{+\infty} \delta(\omega - \omega^*) S_g(\omega^*, v, \mu) d\omega^* = S_g(\omega, v, \mu) \quad (47)$$

where  $\delta(\cdot)$  is the Dirac delta function. Thus the one-dimensional global lift spectrum becomes

$$S_{L_G}(\omega) = \iint_{-\infty}^{+\infty} \Phi_2^2(v) \Phi_3^2(\mu) S_g(\omega, v, \mu) dv d\mu \quad (48)$$

where

$$\begin{aligned} \Phi_2(v) &= \left| \int_0^{H_2} \int_0^{H_1} s(x_1)s(x_2) e^{iv(x_1 - x_2)} dx_1 dx_2 \right|^{1/2} \\ &= \left| \int_0^H s(x) e^{ivx} dx \right| \end{aligned} \quad (49)$$

$$\begin{aligned}\Phi_3(\mu) &= \left| \sum_{n=1}^N \sum_{m=1}^N r_m r_n e^{\mu(z_m - z_n)} \right|^{1/2} \\ &= \left| \sum_{n=1}^N r_n e^{i\mu z_n} \right|\end{aligned}\quad (50)$$

and  $S_d$  is given by equation (35).

$\Phi_2$  and  $\Phi_3$  can be thought of as the spanwise and vane-to-vane correlation functions, respectively. Their effect is to attenuate the lift and drag forces when vane dimensions become large compared to the turbulent velocity scale. Alternately, in the limit as the scale of the turbulent velocity eddies goes to infinity ( $v$  and  $\mu$  tend to zero), a quasi-steady state situation occurs and  $\Phi_2$  and  $\Phi_3$  go to their maximum values. The effect of  $\Phi_2$  and  $\Phi_3$  as a function of nondimensional wave number can be seen in figures 4 and 5.

The approach developed in this section is also applicable to global dynamic drag. Using this approach, the one-dimensional global drag spectrum can be shown as

$$S_{D_G}(\omega) = \int_{-\infty}^{+\infty} \Phi_2^2(v) \Phi_3^2(\mu) S_d(\omega, v, \mu) dv d\mu \quad (51)$$

where  $S_d$  is given by equation (36).

It should be noted that the power spectra of equations (48) and (51) have been left in the two-sided format ( $-\infty < \omega < \infty$ ). One-sided spectra ( $0 < \omega < \infty$ ), used for many applications, can easily be derived from these simply by doubling the spectral values for positive frequencies.

The squares of the rms lift and drag are subsequently determined by integrating their respective power spectra over the entire frequency range, such that

$$\sigma_{L_G}^2 = \int_{-\infty}^{+\infty} S_{L_G}(\omega) d\omega \quad (52)$$

$$\sigma_{D_G}^2 = \int_{-\infty}^{+\infty} S_{D_G}(\omega) d\omega \quad (53)$$

## LOCAL LOADS

Local dynamic loads can be determined by incorporating two simplifying assumptions into the global analysis. First, because local loads are for one vane only, the cross-stream velocity profile is not necessary and the normalized vane-to-vane correlation function ( $\phi_3/N$ ) becomes unity for all values of wave number  $\mu$  (see fig. 5). Secondly, integration done in the vertical direction need only be done for the small vane section of interest and not for a whole vane.

## TURBULENCE SPECTRA

In order to estimate the sectional dynamic lift and drag power spectra of equations (35) and (36), it was necessary to find analytic forms for the lateral, axial, and cross-velocity power spectra. For simplicity, a turbulence model was chosen that assumed the turbulent velocities were homogeneous, isotropic and Gaussian. It was assumed, however, that small differences between the axial and the lateral rms velocity components could be accounted for by adjusting these constants in the model. Using these assumptions, the 3-D power spectra for turbulence can be expressed in terms of a basic energy spectrum function  $E(v^*)$  by the following equation (refs. 6 and 7)

$$\theta_{ij} = \frac{E(v^*)}{4\pi v_*^4} (v_*^2 \delta_{ij} - v_i v_j) \quad (54)$$

where  $E(v^*)$  is a scalar function that describes the turbulent energy density as a function of the wave number magnitude  $v^*$ ,  $v_i$  are the wave number magnitude components ( $i = 1$  to 3),  $\delta_{ij}$  is the Kronecker delta, and

$$v^* = |\vec{v}| = (v_1^2 + v_2^2 + v_3^2)^{1/2} \quad (55)$$

Two-dimensional and one-dimensional spectra and the integrated rms can be derived as follows

$$\psi_{ij}(v_1, v_2) = \int_{-\infty}^{+\infty} \theta_{ij} dv_3 \quad (56)$$

$$\phi_{ij}(v_1) = \int_{-\infty}^{+\infty} \psi_{ij} dv_2 \quad (57)$$

$$\sigma_i^2 = \int_{-\infty}^{+\infty} \phi_{ii} dv_1 \quad (58)$$

For the axial and vertical directions important to our analysis, directions 1 and 3 respectively, equation (54) becomes

$$\theta_{11}(\vec{v}) = \frac{E(v^*)}{4\pi v_*^4} (v_2^2 + v_3^2) \quad (59)$$

$$\theta_{33}(\vec{v}) = \frac{E(v^*)}{4\pi v_*^4} (v_1^2 + v_2^2) \quad (60)$$

$$\theta_{13}(\vec{v}) = \frac{E(v^*)}{4\pi v_*^4} (-v_1 v_3) \quad (61)$$

$\theta_{11}$  is the axial,  $\theta_{33}$  is the vertical, and  $\theta_{13}$  is the cross spectrum of the turbulence. A form of the energy spectrum function that applies to wind tunnel turbulence (ref. 8) is

$$E(v^*) = \sigma_i^2 \frac{8L}{\pi} \frac{L^2 v_*^4}{(1 + L^2 v_*^2)^3} \quad (62)$$

where  $\sigma_i$  is the rms velocity fluctuation and  $L$  is the characteristic length scale for axial turbulence. Plugging this function into equations (59)-(61) and letting  $\sigma$  vary between the directions yields

$$\theta_{11} = \sigma_1^2 \frac{2L^5}{\pi^2} \frac{v_2^2 + v_3^2}{(1 + L^2 v_*^2)^3} \quad (63)$$

$$\theta_{33} = \sigma_3^2 \frac{2L^5}{\pi^2} \frac{v_1^2 + v_2^2}{(1 + L^2 v_*^2)^3} \quad (64)$$

$$\theta_{13} = \sigma_1 \sigma_3 \frac{2L^5}{\pi^2} \frac{(-v_1 v_3)}{(1 + L^2 v_*^2)^3} \quad (65)$$

Performing the integrations necessary to determine the one-dimensional velocity spectra of equation (57) yields

$$\phi_{11} = \sigma_1^2 \frac{L}{\pi} \frac{1}{(1 + L^2 v_1^2)} \quad (66)$$

$$\phi_{33} = \sigma_3^2 \frac{L}{2\pi} \frac{(1 + 3L^2 v_1^2)}{(1 + L^2 v_1^2)^2} \quad (67)$$

$$\phi_{13} = 0 \quad (68)$$

Since the one-dimensional cross spectra in equation (68) is identically equal to zero, it follows that the cross-spectral components of equations (35) and (36) will not contribute to the load spectra in equations (48) and (51), implying that the loading due to axial and vertical turbulence are statistically independent.

For this analysis, the wave number components are equivalent to

$$v_1 = \omega/V \quad (69)$$

$$v_2 = v \quad (70)$$

$$v_3 = \mu \quad (71)$$

The turbulence spectra can now be put in the functional form required for equations (35) and (36)

$$S_u(\omega, v, \mu) = \frac{1}{V} \theta_{11}(\omega/V, v, \mu) \quad (72)$$

$$S_w(\omega, v, \mu) = \frac{1}{V} \theta_{33}(\omega/V, v, \mu) \quad (73)$$

If a characteristic "break" frequency is then defined such that  $\Omega_b = V/L$ , these equations reduce to

$$S_u(\omega, v, \mu) = \sigma_u^2 \frac{2\Omega_b V^2}{\pi^2} \frac{(vV)^2 + (\mu V)^2}{(\Omega_b^2 + (vV)^2 + (\mu V)^2 + \omega^2)^3} \quad (74)$$

$$S_w(\omega, v, \mu) = \sigma_w^2 \frac{2\Omega_b V^2}{\pi^2} \frac{(vV)^2 + \omega^2}{(\Omega_b^2 + (vV)^2 + (\mu V)^2 + \omega^2)^3} \quad (75)$$

These final two equations for the turbulent velocity spectra can now be substituted into equations (35) and (36). Note that these spectra can be completely described with just three experimentally measured quantities, 1) the break frequency, 2) the rms velocity, and 3) the mean flow velocity.

## PHYSICAL SIGNIFICANCE OF BREAK FREQUENCY

The one-dimensional axial turbulent velocity power spectrum is derived by integrating equation (74)

$$\begin{aligned}
 S_u(\omega) &= \iint_{-\infty}^{+\infty} S_u(\omega, v, \mu) dv d\mu \\
 &= \sigma_u^2 \frac{\Omega_b}{\pi} \frac{1}{\Omega_b^2 + \omega^2} \quad (76)
 \end{aligned}$$

From this latter equation it follows that

$$\frac{S_u(\omega = \Omega_b)}{S_u(\omega = 0)} = \frac{1}{2} \quad (77)$$

Thus, the characteristic "break" frequency  $\Omega_b$  is the frequency on the one-dimensional axial turbulence spectrum where the power is equal to one-half of the value at  $\omega = 0$ .

## RESULTS

Utilizing equations (31), (35), (36), (49), (50), (74), and (75), equations (48) and (51) can be numerically integrated to give estimates for dynamic lift and drag. The parameters whose values must be prescribed in order to integrate these equations, together with actual values for a typical case (vane set 1 of the NFAC), are listed in tables 1 and 2. Some of these parameters come directly from full-scale vane set geometry ( $c, H, Z, N, \theta_1$ ), some from extrapolations of full-scale data ( $\beta_1, \rho$ ), some from small-scale model data ( $n_2, V_m, \beta_2$ , velocity profiles), and others from more complete data gathered at other large wind tunnel facilities ( $\Omega_b, TI_w, TI_u$ ). Justifications for the use of these inputs and complete loads results for the entire NFAC are being published separately. Predicted global lift and drag spectra and rms loads for vane set 1 are shown in figures 6 and 7.

The global loads estimates from this analysis include four factors not found in simpler methods:  $T$ ,  $\Phi_2$ ,  $\Phi_3$ , and the velocity profiles. It is therefore of some interest to determine how much effect each of these factors has on the final results. By neglecting all of them, the loads equations revert to their simplest form: quasi-steady aerodynamics, perfectly correlated turbulence, and uniform velocity profiles. The global lift and drag spectra for the case of vane set 1 are shown in figures 8 and 9. The individual effects of  $T$ ,  $\Phi_2$ , and  $\Phi_3$  can then be

seen by comparing the rms loading for this simple baseline case with results obtained by independently incorporating each factor into the loads equations. The results are presented in table 3. It is apparent that each one of these factors has a significant attenuating effect on the dynamic loads estimates. If these effects are combined, the lift and drag spectra of figures 10 and 11 can be calculated. If the appropriate velocity profiles are then included, the spectra of figures 6 and 7 are once again derived. It should be noted that by incorporating all of these effects, the rms lift estimate has been reduced by a factor of 11 when compared to the baseline case (table 3). A similar attenuation factor of 8.7 is observed for rms drag.

The input parameters required to estimate local loads are nearly identical to those of the global loads case. Simplifications do occur, however, since velocity profiles are neglected and integration is done over one small vane section. Examples of lift and drag spectra and rms loading for a 3.47-m section of vane set 1 are shown in figures 12 and 13.

#### CONCLUDING REMARKS

An analytical method has been developed to estimate the unsteady aerodynamic forces caused by turbulence on turning vane cascades. It is a refinement of the quasi-steady, perfectly correlated approach and includes correlation and unsteady aerodynamic effects. The use of this method results in significant attenuation of dynamic loads estimates relative to quasi-steady predictions, especially at higher frequencies. A typical example from one vane set in the NFAC shows attenuation factors of 11 and 8.7 for global lift and drag, respectively. This attenuation could be important since overestimating the vane set loads could cause the subsequent structural analysis to incorrectly indicate a need for renovation of existing structures.

Although this method is undoubtedly more precise than the simple, quasi-steady, perfectly correlated approach, there has been no experimental confirmation of its accuracy. It is therefore recommended that predictions derived from this analysis be supported by experimental measurements.

## REFERENCES

1. Corsiglia, V. R.; Olson, L. E.; and Falarski, M. D.: Aerodynamic Characteristics of the 40- by 80/80- by 120-Foot Wind Tunnel at NASA Ames Research Center, NASA TM-85946, 1984.
2. Horlock, J. H.: Axial Flow Compressors, Fluid Mechanics and Thermodynamics, Butterworths Scientific Publications, 1958, p. 33.
3. Sears, W. R.: Some Aspects of Non-Stationary Airfoil Theory and its Practical Application. *J. Aero. Sci.*, vol. 8, no. 3, Jan. 1941, pp. 104-108.
4. Greenberg, J. M.: Airfoil in Sinusoidal Motion in a Pulsating Stream. NACA TN-1326.
5. Filotas, L. T.: Theory of Airfoil Response in a Gusty Atmosphere Part II-- Response to Discrete Gusts or Continuous Turbulence, UTIAS Report No. 141, Univ. Toronto, 1969.
6. Etkin, B.: Dynamics of Flight-Stability and Control, John Wiley & Sons, Inc., 1959.
7. Etkin, B.: Dynamics of Atmospheric Flight, John Wiley & Sons, Inc., 1972.
8. Houbolt, J. C.; Steiner, R.; and Pratt, K. G.: Dynamic Response of Airplanes to Atmospheric Turbulence Including Flight Data on Input and Response, NASA TR R-199, 1964.

TABLE 1.- GLOBAL LOADS INPUT FOR VANE SET 1

Parameter	Symbol	Input value
Vane chord	c	1.83 m
Length of one vane	H	20.91 m
Distance along stagger line	Z	46.86 m
Number of vanes in set	N	50
Viscous drag coefficient	$\eta_d$	0.114
Inflow angle between free stream and centerline	$\beta_1$	0.733 rad ( $42^\circ$ )
Outflow angle between free stream and centerline	$\beta_2$	-0.855 rad ( $-49^\circ$ )
Stagger angle	$\theta_1$	0.785 rad ( $45^\circ$ )
Maximum time-averaged velocity	$V_{0_{max}}$	75.74 m/sec
Air density	$\rho$	1.172 kg/m <sup>3</sup>
"Break" frequency	$\Omega_b$	3.0 Hz
Lateral turbulence intensity	$TI_w$	0.156
Axial turbulence intensity	$TI_u$	0.115

TABLE 2.- GLOBAL LOADS INPUT FOR  
VANE SET 1--VELOCITY PROFILES

Vane no.	Cross-stream velocity ratio $r_n$	Vane no.	Cross-stream velocity ratio $r_n$
1	0.579	26	0.653
2	.650	27	.697
3	.721	28	.756
4	.792	29	.798
5	.862	30	.840
6	.922	31	.883
7	.953	32	.925
8	.980	33	.968
9	.988	34	.991
10	.995	35	.997
11	.995	36	1.000
12	.995	37	.999
13	.995	38	.997
14	.995	39	.994
15	.995	40	.992
16	.995	41	.987
17	.993	42	.976
18	.986	43	.965
19	.971	44	.936
20	.947	45	.902
21	.906	46	.863
22	.857	47	.793
23	.809	48	.712
24	.760	49	.623
25	.700	50	.502
Normalized vertical distance, $x/H$		Vertical velocity ratio, $s(x)$	
	0.000		0.000
	.013		.378
	.125		.675
	.225		.885
	.316		.971
	.325		.994
	.471		1.000
	.604		1.000
	.694		.974
	.788		.861
	.863		.715
	.944		.607
	.991		.484
	1.000		.000

TABLE 3.- ATTENUATION DUE TO  $T$ ,  $\phi_2$ ,  $\phi_3$ , AND VELOCITY PROFILES

Case number	Global rms lift estimate	Global rms drag estimate
	Baseline global rms lift estimate	Baseline global rms drag estimate
1. Baseline estimate (neglect $T$ , $\phi_2$ , $\phi_3$ , and velocity profiles)	1.0	1.0
2. With $T$ only	.515	.484
3. With $\phi_2$ only	.467	.469
4. With $\phi_3$ only	.354	.422
5. With $T$ , $\phi_2$ , $\phi_3$	.115	.147
6. With $T$ , $\phi_2$ , $\phi_3$ , and profiles	.091	.114

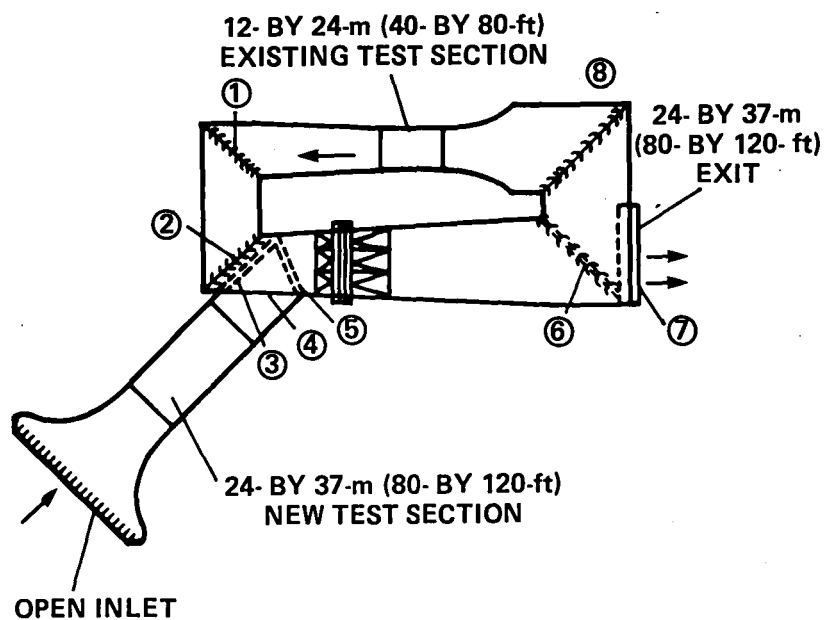


Figure 1.- NFAC showing vane set locations.

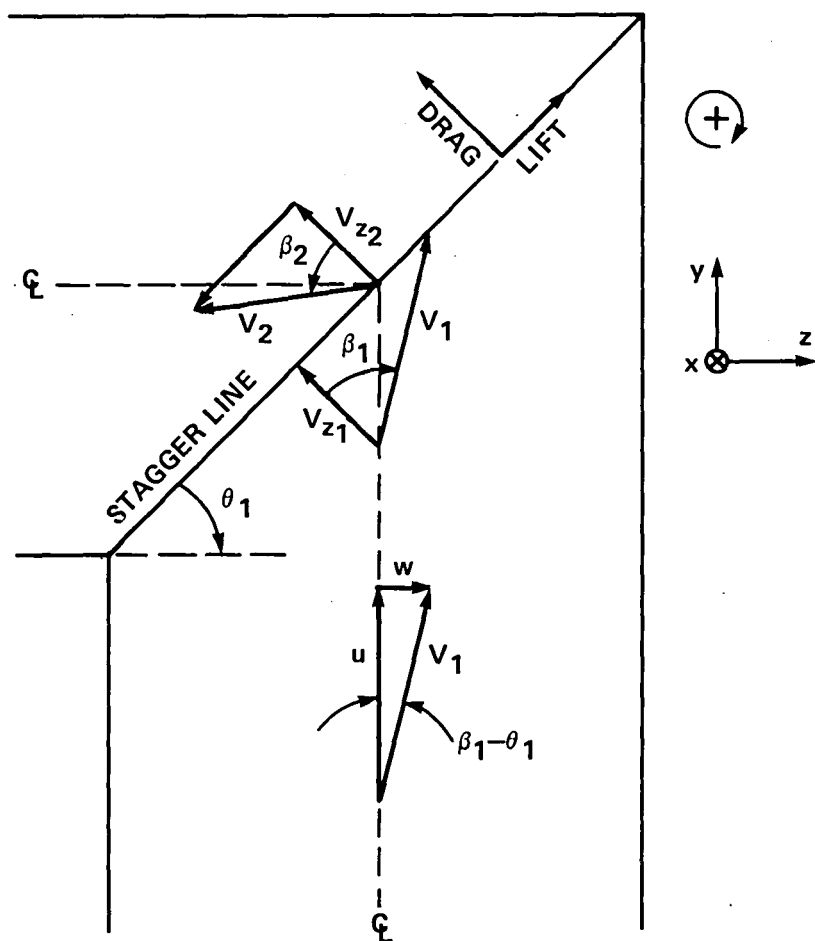


Figure 2.- Definitions and sign conventions for variables.

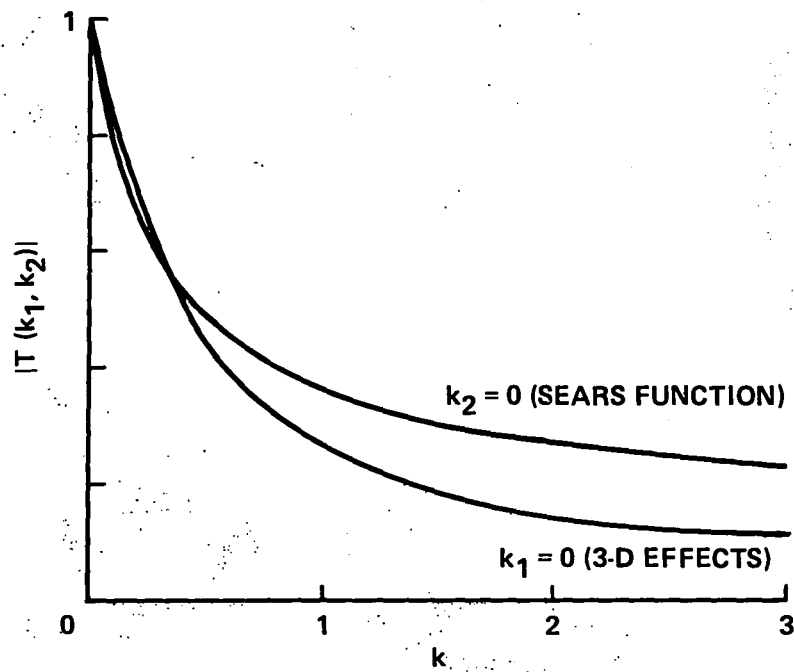


Figure 3.- Extended Sears function vs. reduced frequency.

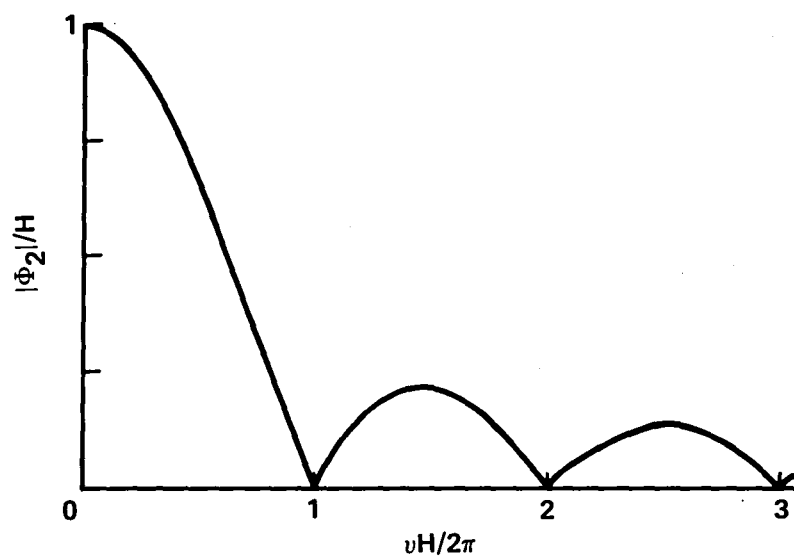


Figure 4.- Spanwise correlation vs. nondimensional wave number for a uniform velocity profile ( $s(x) \equiv 1$ ).

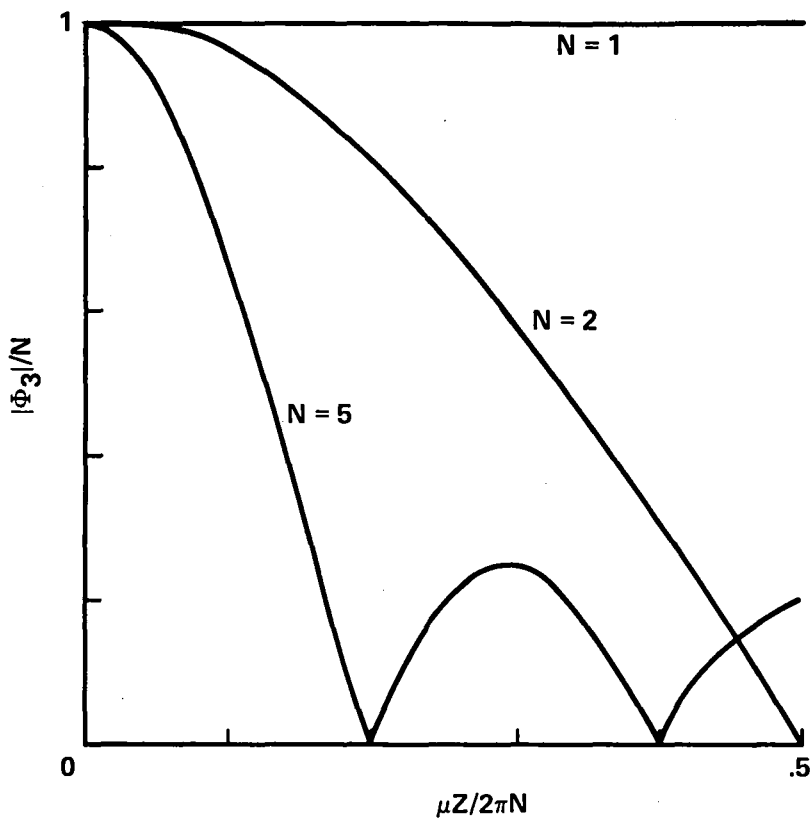


Figure 5.- Vane-to-vane correlation vs. nondimensional wave number for a uniform velocity profile ( $r_n \equiv 1$ ).

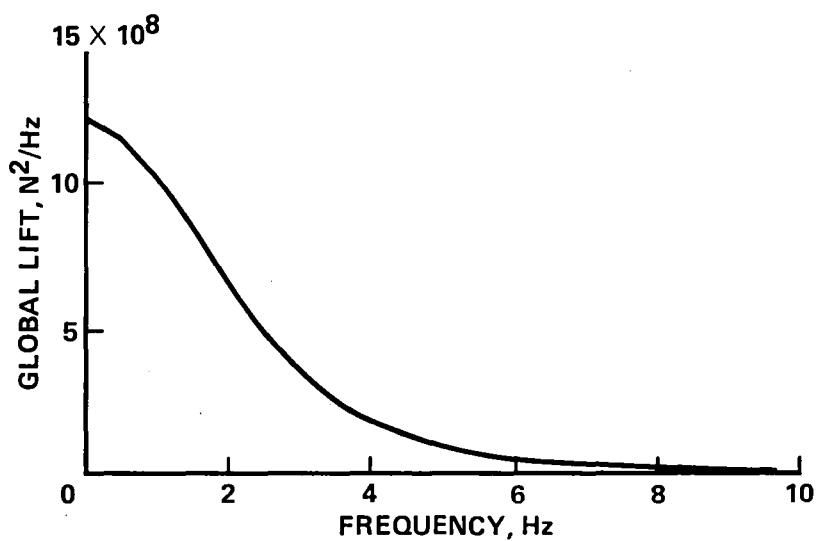


Figure 6.- Global lift spectrum for vane set 1,  $\sigma = 165,000$  N.

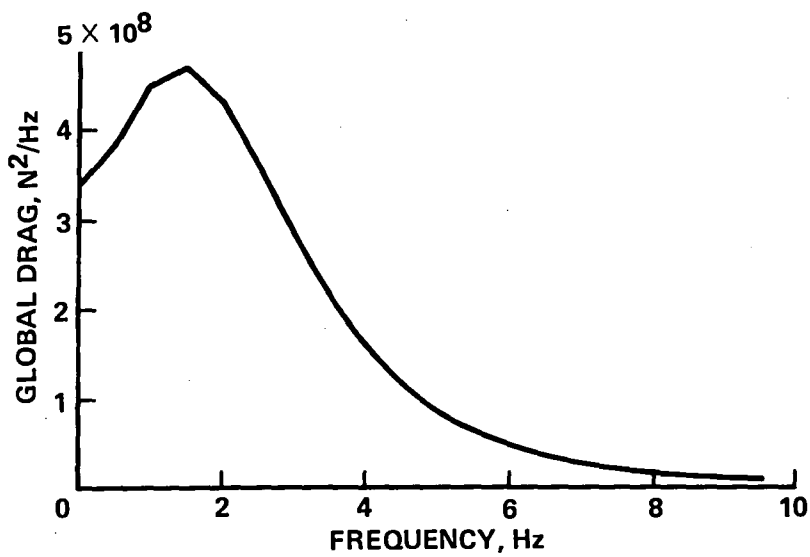


Figure 7.- Global drag spectrum for vane set 1,  $\sigma = 123,200$  N.

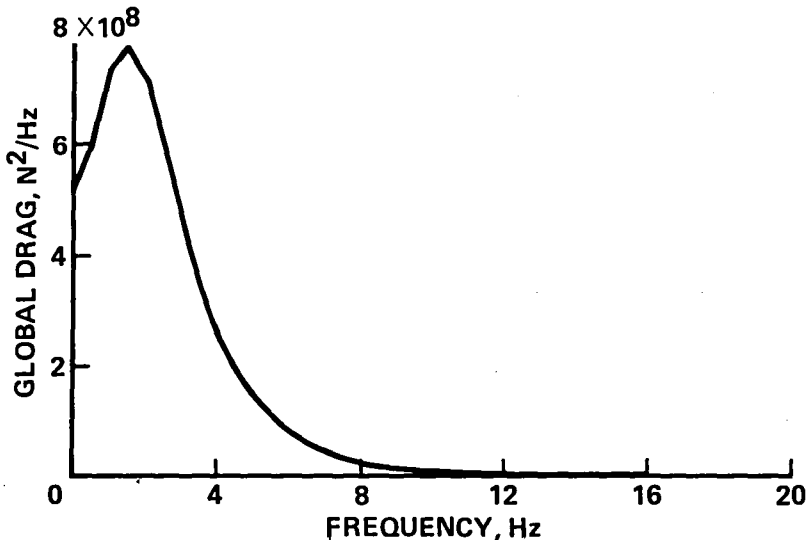


Figure 8.- Global lift spectrum neglecting  $T$ ,  $\phi_2$ ,  $\phi_3$ , and velocity profiles,  $\sigma = 1,810,000$  N.

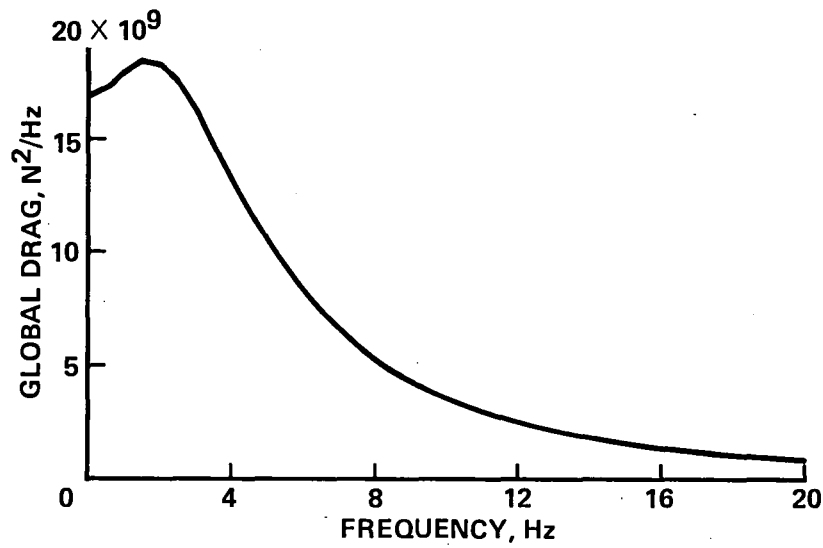


Figure 9.- Global drag spectrum neglecting  $T$ ,  $\phi_2$ ,  $\phi_3$ , and velocity profiles,  $\sigma = 1,076,500$  N.

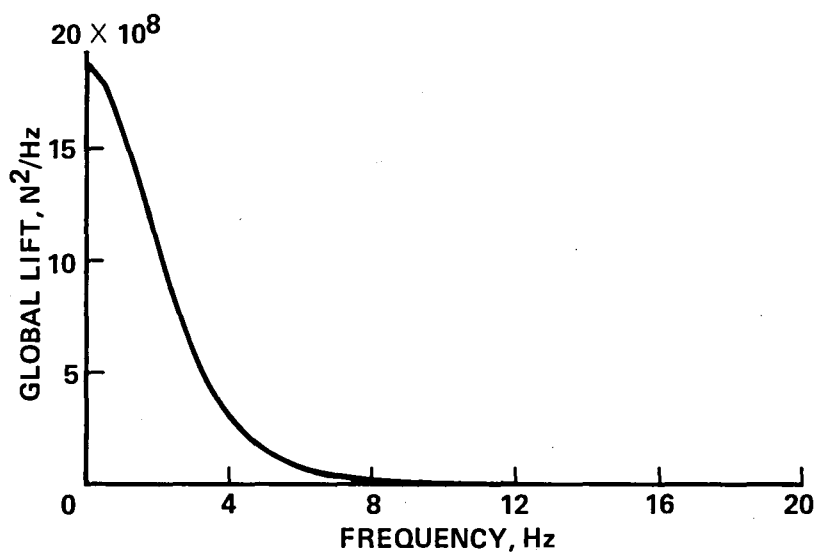


Figure 10.- Global lift spectrum neglecting velocity profiles,  $\sigma = 208,200$  N.

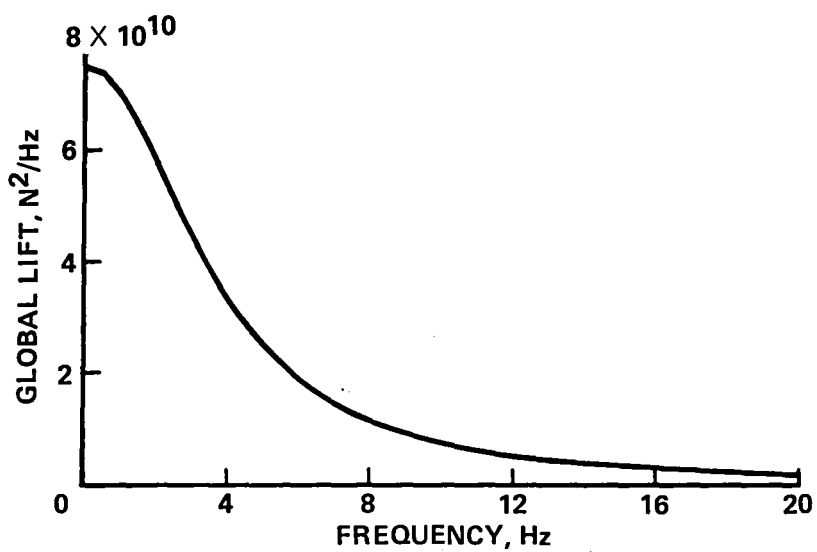


Figure 11.- Global drag spectrum neglecting velocity profiles,  
 $\sigma = 158,400$  N.

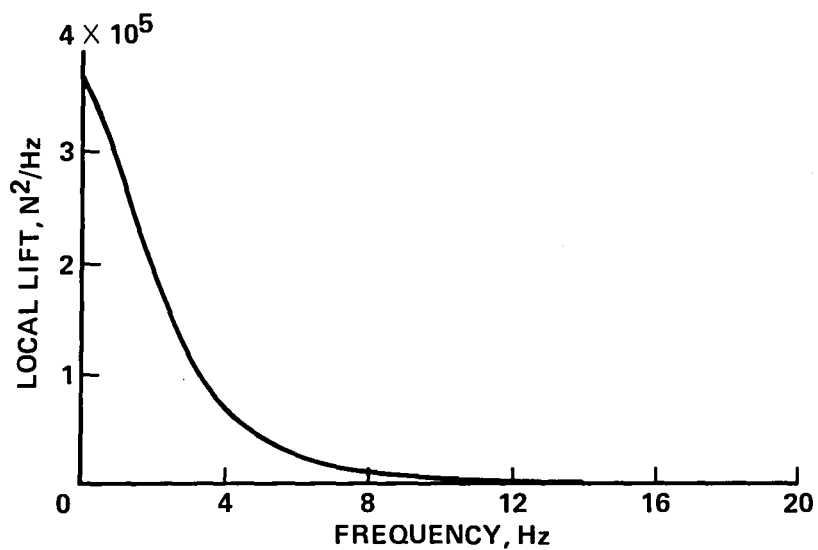


Figure 12.- Local lift spectrum for 3.47 m section of vane set 1,  
 $\sigma = 2960$  N.

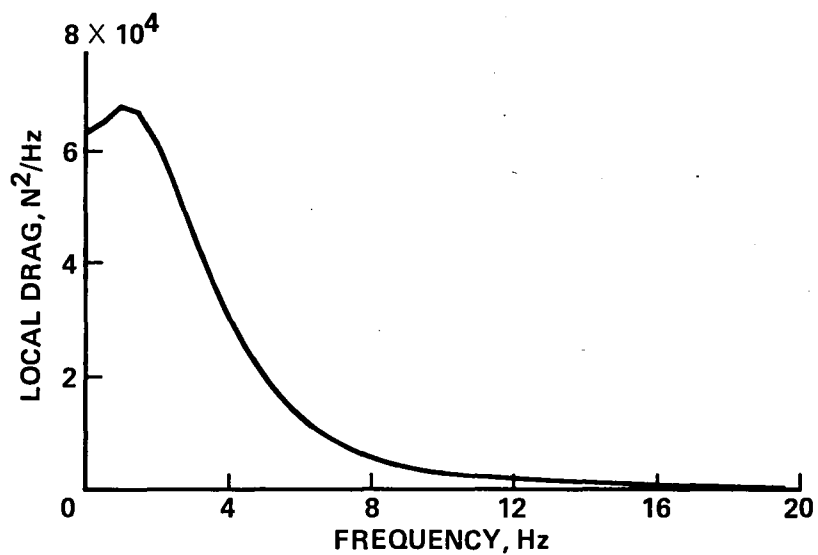


Figure 13.- Local drag spectrum for 3.47 m section of vane set 1,  
 $\sigma = 1645$  N.

1. Report No. NASA TM-86701	2. Government Accession No.	3. Recipient's Catalog No.	
4. Title and Subtitle <b>ESTIMATING UNSTEADY AERODYNAMIC FORCES ON A CASCADE IN A THREE-DIMENSIONAL TURBULENCE FIELD</b>		5. Report Date <b>March 1985</b>	
		6. Performing Organization Code	
7. Author(s) <b>Thomas R. Norman and Wayne Johnson</b>		8. Performing Organization Report No. <b>85166</b>	
9. Performing Organization Name and Address <b>Ames Research Center Moffett Field, CA 94035</b>		10. Work Unit No. <b>T-4523</b>	
		11. Contract or Grant No.	
12. Sponsoring Agency Name and Address <b>National Aeronautics and Space Administration Washington, DC 20546</b>		13. Type of Report and Period Covered <b>Technical Memorandum</b>	
		14. Sponsoring Agency Code <b>505-42-11</b>	
15. Supplementary Notes <b>Point of Contact: Thomas R. Norman, Ames Research Center, MS 247-1, Moffett Field, CA 94035, (415)694-6096 or FTS 464-6096</b>			
16. Abstract  <b>An analytical method has been developed to estimate the unsteady aerodynamic forces caused by flow field turbulence on a wind tunnel turning-vane cascade system (vane set). This method approximates dynamic lift and drag by linearly perturbing the appropriate steady-state force equations, assuming that the dynamic loads are due only to free-stream turbulence and that this turbulence is homogeneous, isotropic, and Gaussian. Correlation and unsteady aerodynamic effects are also incorporated into the analytical model. Using these assumptions, equations relating dynamic lift and drag to flow turbulence, mean velocity, and vane set geometry are derived. From these equations, estimates for the power spectra and rms (root-mean-squared value, <math>\sigma</math>) loading of both lift and drag can be determined.</b>			
17. Key Words (Suggested by Author(s)) <b>Wind tunnels Unsteady aerodynamics Cascade aerodynamics Analytical method</b>		18. Distribution Statement <b>Unlimited</b>  <b>Subject Category - 02</b>	
19. Security Classif. (of this report) <b>Unclassified</b>	20. Security Classif. (of this page) <b>Unclassified</b>	21. No. of Pages <b>30</b>	22. Price* <b>A03</b>

**End of Document**